"Salted Silica": Sol-Gel Chemistry of Silica under Hypersaline Conditions

(Article begins on next page)

13 May 2024

"Salted silica": Sol-gel chemistry of silica under hypersaline conditions

Roberto Nisticò[a,b], Giuliana Magnacca[a], Markus Antonietti[b], and Nina Fechler[b,*]

[1] University of Torino, Department of Chemistry and NIS Research Centre, Via P. Giuria 7, 10125 Torino, Italy
[2] Max Planck Institute of Colloids and Interfaces, Department of Colloid Chemistry, Am Mühlenberg 1, 14424 Potsdam-Golm, Germany
* Author to whom correspondence should be addressed.

Abstract
In a facile one-step approach, high surface area mesoporous silica powders are synthesized using ordinary salts for pore and morphology control during the sol-gel process. Applying tetraethyl orthosilicate (TEOS) as a reference system, the addition of high salt loads such as NaCl and $ZnCl_2$ results in highly increased surface areas of up to 750 m^2 g^{-1}, predominantly in the mesopore range Besides the surface area, the pore volume and the pore size can be controlled by the salt amount as well as the salt nature, reaching values of 1.1 cm^3 g^{-1} and 14 nm, respectively. Compared to standard processes, the herein presented synthesis is extremely simple: it only comprises the dissolution of TEOS and the respective salt in 1 M HCl, followed by solvent evaporation, salt removal through simple washing with water and drying. This way, no special equipment is required, no organic templates are to be employed, and the overall approach is highly efficient and sustainable.

Keywords: Mesoporous materials; Salt-templating; Salting-in effect; Silica; Sol-gel synthesis.

1. Introduction

One of the high arts of materials chemistry is the precise control of matter on the nanometer scale. For this reason, the search for new methods became a fundamental and important research field, and until today several approaches have been developed and are successful on the market. Some prominent examples are sol-gel processes, hard and soft templating methods or a combination of them. Since the 1990s, and in particular with the early works on the templating action of surfactants and block copolymers on silica,[1–3] a progressive interest towards the development of mesoporous materials is to be noted.[4,5] Thanks to the intrinsic self-assembly properties of amphiphiles, different porosities (in terms of shape and size) can be obtained by organic supramolecular templating, most prominently of diverse oxides such as silicas and zeolites.[6,7] Indeed, the use of organic templates allows for the production of an extreme variety of inorganic structures that already found application in many fields. In particular, mesoporous materials are used as catalysts (both as shape-selective catalytic site and/or catalyst supports), as micro- and nanoreactors, molecular sieves and templates, optical materials, chemical sensors, dielectrics, size-selective membranes, energy-storage materials and selective adsorbents, just to name a few.[8–10]

Soft chemistry is a very common initial step for the generation of such materials.[11] This approach is based on the coexistence of organic and inorganic species and, since this field is still under exploration, a lot of different strategies have been proposed in order to obtain well-ordered and highly-organized materials.[13–15] Here, through the mediation of electrostatic, hydrogen-bonding, covalent and van der Waals interactions, amphiphiles organize into supramolecular arrays, around which the inorganic network then growth.[16] Another approach is the formation of inorganic nanoparticles by polymerization and/or precipitation in solution, or inside micelles and vesicles which allows for the realization of complex hierarchical materials.[17] However, one of the main problems concerning the soft templating process is the template removal afterwards. Until now, this is accomplished through solvent extraction or thermal decomposition of the organic part.[18] On the one hand, this requires organic solvents and on the other hand the template cannot be reused and

also often leaves undesired residues. Therefore, research efforts are to be made to find more convenient and sustainable structuring processes.[19–21]

Very recently, a new pathway for the production of micro- and mesoporous carbons was presented where simple inorganic salts were used as templates.[22,23] In particular, within this process named "salt-templating", concentrated solutions or even melts of ordinary inorganic salts are mixed with a carbon precursor which is condensed and scaffolded in the presence of the liquid salt phase at elevated temperatures. The materials possess high surface areas with pore sizes and shapes corresponding to the molecules, salt clusters and their percolation structures.[22] Salts are then easily removed by simple washing with water, thus a simple closed-loop process including salt recycling can be imagined. Even monolithic porous carbon aerogels were accessible, which were stable enough to be dried from water without employing supercritical processes.[23]

In the present work, the salt templating approach is further extended to the generation of porous oxides, here in particular to the synthesis of mesoporous silica. Using TEOS as model system, it will be shown that the surface area and pore size of the resulting silica can be tuned through both, the salt amount and salt nature. Furthermore, main variables which control the pore formation will be discussed. Besides the condensation around salt clusters, the different abilities of the salts to stabilize the colloidal system (salting-in effect) and the action as coalescent agent to sharpen the final structures (salting out effect) according to the Hofmeister series,[24] are expected to contribute to the pore formation.[25–27]

2. Results and discussion

For the synthesis of mesoporous silica powders by the salt-templating approach, TEOS was selected as silica precursor. The reaction was conducted in acidic medium (1 M HCl) in order to moderate the polycondensation process. As porogens salts, different chlorides were used where sodium chloride and zinc chloride were chosen as representative systems for a monovalent (Na^+) and divalent (Zn^{2+}) system, respectively. Besides the effect of the valence, the porosity development was also followed for systems containing different amounts of salts. In order to study the generality of the approach as well as how different salt dimensions and properties can change the final structure, lithium chloride, potassium chloride and cesium chloride were also investigated under otherwise fixed optimal conditions. The overall process is summarized in **Scheme 1**.

After dissolution of the respective salt (red) in acid and the addition of TEOS (green) (**Scheme 1 a**), polycondensation reactions were conducted through heating at 50 °C (**Scheme 1 b**). During this process, the silicic network is formed in the presence of the respective inorganic salt and obtained either as a jelly, transparent substance in case of salting-in ions, or as whitish, particulate dispersion in case of salting-out ions (**Scheme 1 c**, green). Afterwards, the template is very easily removed just by washing the system with water (**Scheme 1 d**). The products are named SaSi-X-Y, where SaSi stands for salt/silica, X for the type of cation of the template salt and Y for the salt/TEOS mass ratio in the synthesis.

Wide angle X-ray scattering (**Figure SI-1**) patterns of the washed products show the typical broad peak of amorphous silica at $2\theta \approx 23°$. The absence of additional peaks indicates the effective removal of the inorganic salt species. For SaSi-Zn-0.5 and for all the NaCl templated samples, another peak at $2\theta \approx 18°$ is also found. This reflection could be due to lowly ordered water micropores.

Already the macroscopic appearance of a reference sample synthesized without any salt (SaSi-0–0) and samples prepared with NaCl and $ZnCl_2$ (SaSi-Na-2 and SaSi-Zn-2) clearly points to different material properties. In the salt-containing cases fluffy powders are obtained, whereas the reference sample appears rather dense. Transmission and scanning electron microscopy (TEM and SEM) confirm this observation and only show an irregular, denser morphology for the reference material (**Figure 1**, left).

Instead, the salt templated, washed products (**Figure 1**, middle and right) reveal low-density and interconnected structures which are constituted of very small nanoparticles of around 10 nm in

diameter. This already illustrates the possibility to take influence on the silica structure just by the presence of an ordinary salt. In the case of the $ZnCl_2$ templated materials, increasing the amount of salt results in an increased softness and fluffiness of the final silica powders that is the primary particles are getting smaller and more interlinked (**Figure SI-2**, right). This behavior is different for NaCl templated powders, where the materials reach a maximum fluffiness but then denser structures are formed again at very high salt amounts (**Figure SI-2**, left). This is attributed to the difference in the salting-in ($ZnCl_2$) and salting-out (NaCl) ability, according to the Hofmeister series (**Scheme SI-1**) of the two salts, which will be discussed below together with the gas sorption data.

In order to determine morphological variations in more detail also on the nanometer scale, nitrogen sorption measurements were performed for the two series of NaCl and $ZnCl_2$ templated silica (**Figure 2**).

In all cases, the salt addition results in an increased nitrogen uptake compared to the reference material which indicates an increased porosity. The actual apparent surface areas (**Table SI-1**) and pores size distributions (**Figure 2** right) were determined by applying the Brunauer–Emmett–Teller (BET) model and the Non-Local Density Functional Theory (NLDFT) equilibrium model method for slit pores, respectively. It can be seen, that the apparent surface areas significantly increase due to salt-templating, with values ranging from 500 $m^2\,g^{-1}$ up to 700 $m^2\,g^{-1}$. In the NaCl series (**Figure 2**, top), the addition of 0.5 g NaCl only increases the small pores of the system but leaves essentially the curve features unchanged, that is here presumably single salt pairs stabilize solvent pores within the silica, but no bigger morphological changes take place. For higher NaCl concentrations, pronounced mesopore development and pore expansion to pore diameters of 2.5–8 nm are observed. This means, that at those concentrations the salt-system demixes into a second, porogenic phase, which however is confined by the polycondensation structure. Within the NaCl series, at very high concentrations, the pore volume decreases again, indicating a "salting-out" of the structures at too early phases of the silica polycondensation. This is in accordance to the already mentioned densification of the materials at high NaCl levels and supports the results obtained from SEM measurements (**Figure SI-2**).

In the $ZnCl_2$ series, the addition of up to 2 g salt immediately induced the formation of mesopores of 8 nm in diameter, while the pore volume increases with the amount of salt, reaching a maximum value of 1.05 $cm^3\,g^{-1}$ (**Table SI-1**). Just for the highest amount of 10 g $ZnCl_2$, the pore size further increases to 14 nm diameter, however, the pore volume is not reduced as in the case of NaCl but still slightly increases.

In general, this means that at lower salt concentrations, the systems can stay in a homogeneous state throughout the reaction, and the salts only stabilize the small solvent pores being present also in the salt-free default sample. At higher concentrations, the salts promote system-demixing and form "salt-pools" the size of which is determined by the onset of demixing in relation to the degree of condensation. In fact, for Na^+ and K^+ (salting-out ions) larger pores are obtained due to an earlier onset of demixing. On the contrary, salting-in ions (such as Zn^{2+}) allow to obtain higher mesopore volumes with a more defined pore size distribution. This is because they tend to stabilize the forming network keeping the whole system homogeneous over a longer period which only changes at very high salt concentrations. Therefore, increasing the salt amount of salting-in ions leads to a continuous increase of the mesoporosity and pore volume, because extra added salt is really used as a porogen (**Table SI-1**).

To further test the influence of the salt nature also between other monovalent cations and the generality of the approach, a series using different chloride salts (Li^+, Na^+, K^+, Cs^+, Zn^{2+}) was prepared at an optimized, fixed salt concentration (SaSi-X-2). It is important to notice that in the case of SaSi-Li-2 and SaSi-Cs-2 after solvent evaporation at 50 °C the crude samples were obtained as transparent gels, exactly as in the case of the salting-in salt $ZnCl_2$ mentioned above. This already hints to a higher stabilization of the structures compared to SaSi-Na-2 and SaSi-K-2 which were obtained as white powders. Also the SEM micrographs of SaSi-Li-2 and SaSi-Cs-2 reveal finer

structures for the washed materials (**Figure SI-3**) which is in accordance to their stronger salting-in effect.

Nitrogen sorption measurements of the final products show a similar systematic dependency of the porosity on the salt type (**Figure 3**).

In all cases, a hysteresis can be observed which points to the formation of mesopores. The isotherms obtained for SaSi-Na-2 and SaSi-K-2 show comparable shapes, yet with a lower pore volume in the case of KCl due to a stronger salting-out effect of this salt. Already macroscopically, SaSi-Li-2 and SaSi-Cs-2 are fluffier and much finer powders than SaSi-Na-2 and SaSi-K-2 which points to smaller structures of the two former silicas. This is indeed confirmed by nitrogen sorption measurements where for both SaSi-Li-2 and SaSi-Cs-2 the hysteresis closes at lower relative pressures than for SaSi-Na-2 and SaSi-K-2. This together with the pore size distributions (**Figure 3** right) confirms the presence of smaller pores if salts with a higher salting-in effect, i.e. LiCl and CsCl, are used as porogen. Additionally, slightly smaller pores are obtained for SaSi-Li-2 than for SaSi-Cs-2 which is assumed to originate from a weaker salting-in effect of Cs^+. It is important to emphasize that if the salting in/out ability would be the only influence, then SaSi-Zn-2 should possess the smallest pore size of the whole series. This is, however, not observed, and thus differences in pores sizes may also be due to different ion dimensions, i.e. the smaller pores of SaSi-Li-2 can also result from the smaller size of the Li^+ cation and/or the fact that hydrated Cs^+ ions do not fit into the elemental, local silica cage. Therefore, besides the salting-in/out effect also ion sizes and their hydration states, i.e. "structural stabilizing effects" must be taken into account.

3. Conclusions

In conclusion, a facile and efficient one-pot method to produce mesoporous silicas was presented. The materials were synthesized from TEOS as silica precursor, and ordinary salts such as NaCl or $ZnCl_2$ were used at high concentrations which caused the formation of extra mesoporosity and the coupled introduction of high surface areas. In this approach, the surface area, pore size and pore volume can be controlled simply by varying the amount or nature of the salt. Furthermore, the salt porogen can easily be washed out with water which enables to synthesize and isolate samples without special equipment or safety concerns.

The found systematics was attributed to two main parameters: the ability of a salt to stabilize the forming oxide structures according to the Hofmeister series, i.e. salting-in and salting-out effects, and the size of the hydrated ions. The fact that the synthesis is carried out at relatively low temperatures and that in principle the salt can be recovered afterwards renders the approach sustainable and energy efficient, potentially suitable also in industrial processes. Basically, every miscible salt and even salt mixtures can be applied which enables for precise porosity control. Additionally, also the solvent and precursor can be changed, which opens the door to other (oxide) systems and renders the utilization of salts as structure controlling agents a highly promising toolbox for materials chemistry.

4. Experimental section

4.1 Materials and methods

Tetraethyl orthosilicate (TEOS) was purchased from Aldrich with a purity of >99%. Sodium chloride (from Merck) and zinc chloride (from Sigma–Aldrich) with a purity of >99% were used as reference inorganic salts, thus different amount were investigated (from 0.5 g up to 10 g). Lithium chloride (from Sigma–Aldrich), potassium chloride (from Sigma–Aldrich) and cesium chloride (from Sigma–Aldrich) with a purity of >99% were compared to the reference salts. Hydrochloric acid 1 M (from TitriPUR) was used as acid catalyst. All chemicals were used without further purification.

4.2 Synthesis

In a typical synthesis of silica powders, inorganic salt (0.5 g, 1 g, 2 g or 4–10 g) was firstly dissolved at room temp. in 1 M HCl (15 mL) and afterwards mixed with the silica precursor (1 g). The resulting mixtures were placed into a glass vial and put into an oil bath at 50 °C for 5 d under magnetic stirring. Samples were heated into an oven at 60 °C for several hours.

In order to remove the residual salt porogen, the materials were grinded and washed in water for several hours and finally filtered and dried in vacuo. Sodium chloride templated samples required a second washing step in order to remove completely the salts. A reference material was also prepared in the same way just leaving out the salt in order to evidence the porogens action.

4.3 Physico-chemical characterization

Wide angle X-rays scattering (WAXS)-patterns were measured with a Bruker D8 Advance instrument using Cu-Kα-radiation. Nitrogen sorption measurements were accomplished with N_2 at 77 K after degassing the samples at 150 °C under vacuum for 20 h using a Quantachrome Quadrasorb SI porosimeter. The apparent surface area was calculated by applying the Brunauer–Emmett–Teller (BET) model to the isotherm data points of the adsorption branch in the relative pressure range $p/p_0 < 0.11$ for the microporous and $p/p_0 < 0.3$ for the mesoporous materials. The pore size distribution was calculated from N_2 sorption data using the nonlocal density functional theory (NLDFT) equilibrium model method for slit pores provided by Quantachrome data reduction software Quadra-Win Version 5.05. TEM images were obtained using a Zeiss EM 912Ω instrument. Elemental analysis was accomplished as combustion analysis using a Vario Micro device. SEM images were obtained on a LEO 1550-Gemini instrument after sputtering with platinum.

5. Acknowledgements

References

[1] J. S. Beck, J. C. Vartuli, W. J. Roth, M. E. Leonowicz, C. T. Kresge, K. D. Schmitt, C. T. W. Chu, D. H. Olson, E. W. Sheppard, S. B. McCullen, J. B. Higgins, J. L. Schlenker, **J. Am. Chem. Soc**. 1992, 114, 10834–10843.

[2] C. T. Kresge, M. E. Leonowicz, W. J. Roth, J. C. Vartuli, J. S. Beck, **Nature** 1992, 359, 710–712.

[3] Q. Huo, D. I. Margolese, U. Ciesla, P. Feng, T. E. Gier, P. Sieger, R. Leon, P. M. Petroff, F. Schüth, G. D. Stucky, **Nature** 1994, 368, 317–321.

[4] P. C. A. Alberius, K. L. Frindell, R. C. Hayward, E. J. Kramer, G. D. Stucky, B. F. Chmelka, **Chem. Mater**. 2002, 14, 3284–3294.

[5] D. Zhao, J. Feng, Q. Huo, N. Melosh, G. H. Fredrickson, B. F. Chmelka, G. D. Stucky, **Science** 1998, 279, 548–552.

[6] J. R. Holst, A. I. Cooper, **Adv. Mater**. 2010, 22, 5212–5216.

[7] A.-H. Lu, W.-C. Li, W. Schmidt, F. Schüth, **Microporous Mesoporous Mater**. 2005, 80, 117–128.

[8] K. J. C. van Bommel, A. Friggeri, S. Shinkai, **Angew. Chem. Int. Ed**. 2003, 42, 980–999.

[9] A. Stein, B. J. Melde, R. C. Schroden, **Adv. Mater**. 2000, 12, 1403–1419.

[10] X. Huang, R. G. Weiss, **Langmuir** 2006, 22, 8542–8552.

[11] S. Polarz, B. Smarsly, C. Göltner, M. Antonietti, **Adv. Mater**. 2000, 12, 1503–1507.

[12] G. J. de A. A. Soler-Illia, C. Sanchez, B. Lebeau, J. Patarin, **Chem. Rev**. 2002, 102, 4093–4138.

[13] C. Sanchez, G. J. de A. A. Soler-Illia, F. Ribot, C. Mayer, V. Cabuil, T. Lalot, **Chem. Mater**. 2001, 13, 3061–3083.

[14] M. Tiemann, M. Fröba, **Chem. Mater**. 2001, 13, 3211–3217.

[15] B. Smarsly, S. Polarz, M. Antonietti, **J. Phys. Chem. B** 2001, 105, 10473–10483.

[16] P. Yang, D. Zhao, D. I. Margolese, B. F. Chmelka, G. D. Stucky, **Nature** 1998, 396, 152–155.

[17] G. J. de A. A. Soler-Illia, C. Sanchez, B. Lebeau, J. Patarin, **Chem. Rev**. 2002, 102, 4093–4138.

[18] G. Abellán, A. I. Carrillo, N. Linares, E. Serrano, J. García-Martínez, **J. Solid State Chem**. 2009, 182, 2141–2148.

[19] E.-P. Ng, J.-Y. Goh, T. C. Ling, R. R. Mukti, **Nanoscale Res. Lett**. 2013, DOI: 10.1186/1556–276X-8–120.

[20] N. Baccile, F. Babonneau, B. Thomas, T. Coradin, **J. Mater. Chem**. 2009, 19, 8537–8559.

[21] F. Cuoq, A. Masion, J. Labille, J. Rose, F. Ziarelli, B. Prelot, J. Y. Bottero, **Appl. Surf. Sci**. 2013, 266, 155–160.

[22] N. Fechler, T.-P. Fellinger, M. Antonietti, **Adv. Mater**. 2013, 25, 75–79.

[23] N. Fechler, S.-A. Wohlgemuth, P. Jäker, M. Antonietti, **J Mater. Chem. A** 2013, DOI: 10.1039/C3TA10674H.

[24] E. Leontidis, **Curr. Opin. Colloids Interf. Sci**. 2002, 7, 81–91.

[25] W. L. Queen, S.-J. Hwu, S. Reighard, **Inorg. Chem**. 2010, 49, 1316–1318.

[26] N. Schwierz, D. Horinek, R. R. Netz, **Langmuir** 2013, 29, 2602–2614.

[27] M. G. Cacace, E. M. Landau, J. J. Ramsden, **Quart. Rev. Biophys**. 1997, 3, 241–277.
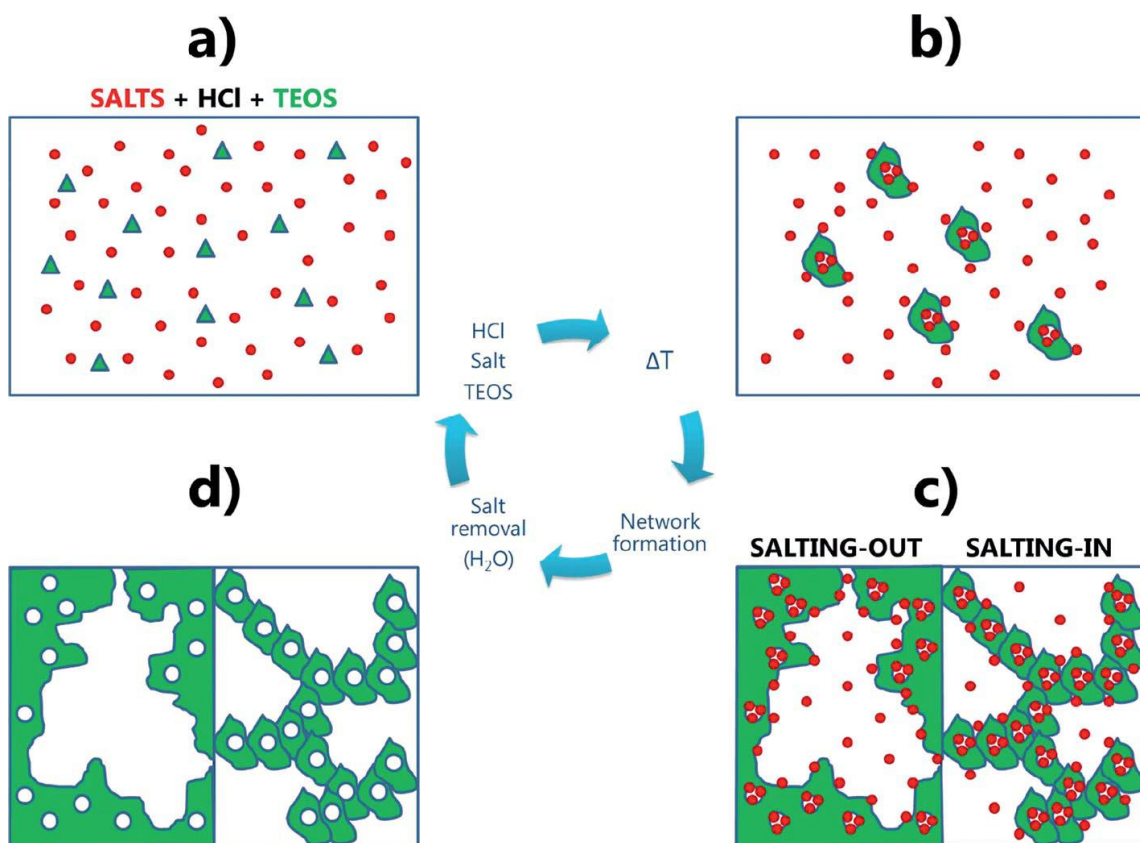
Scheme 1. Reaction steps during salt-templating of mesoporous silica from TEOS under hypersaline conditions. a) Dissolved salt (red) in 1 M HCl and TEOS (green), b) sol-gel process with onset of silica formation (green), c) growth of an extended silica network (green) in salt presence for salting-in and salting-out salts and d) final silica after aqueous removal of the structuring salt.
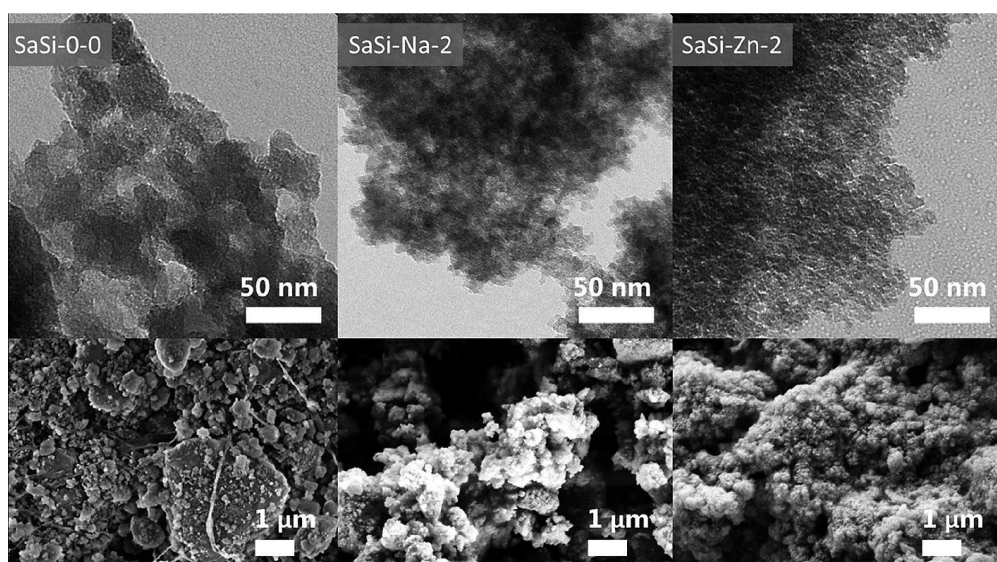
Figure 1. TEM (upper row) and SEM pictures (lower row) of washed silica powders: salt-free reference SaSi-0–0 (left), salt-templated by NaCl (SaSi-Na-2, middle) and $ZnCl_2$ (SaSi-Zn-2, right).
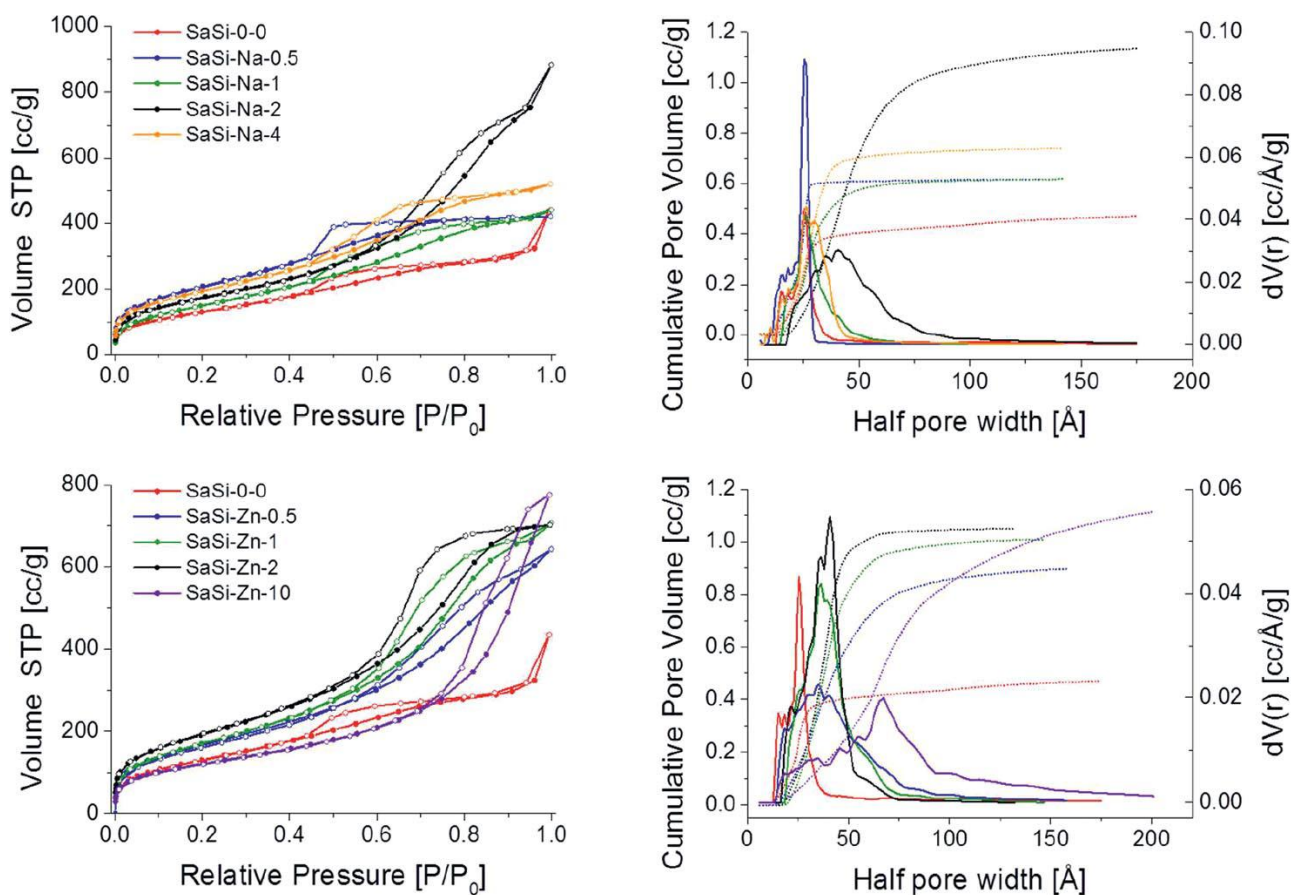
Figure 2. Nitrogen sorption isotherms (left) and pore size distribution (right) of silica powders templated with NaCl (top) and ZnCl₂ (bottom) at varying salt amounts: amount: 0.0 g (red), 0.5 g (blue), 1.0 g (green), 2.0 g (black) 4.0 g (orange) and 10 g (violet).
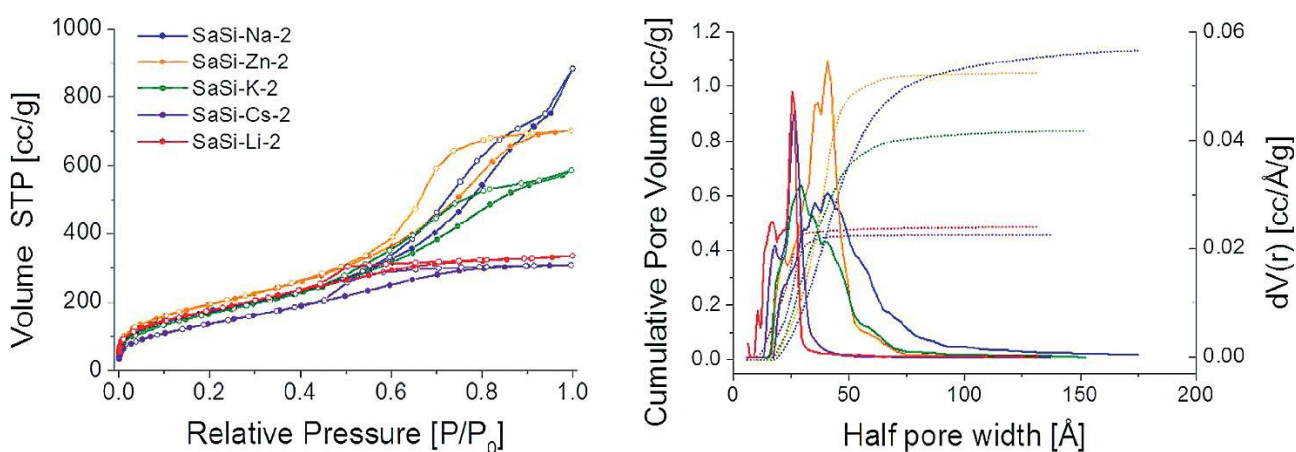
Figure 3. Nitrogen sorption isotherms (left) and pore size distribution (right) of silica powders templated with different types of salt at equal mass ratios: NaCl (blue), ZnCl₂ (orange) KCl (green), CsCl (violet) and LiCl (red).